The Astrophysical Journal, 615:L57–L60, 2004 November 1

HELICITY OF SOLAR ACTIVE REGIONS FROM A DYNAMO MODEL

Arnab Rai Choudhuri and Piyali Chatterjee
Department of Physics, Indian Institute of Science, Bangalore 560012, India; arnab@physics.iisc.ernet.in, piyali@physics.iisc.ernet.in
and
Dibyendu Nandy
Department of Physics, Montana State University, Bozeman, MT 59717-3840; nandi@mithra.physics.montana.edu
Received 2004 August 3; accepted 2004 September 21; published 2004 October 4

ABSTRACT

We calculate helicities of solar active regions based on the idea that poloidal flux lines get wrapped around a toroidal flux tube rising through the convection zone, thereby giving rise to the helicity. Rough estimates based on this idea compare favorably with the observed magnitude of helicity. We use our solar dynamo model based on the Babcock-Leighton α-effect to study how helicity varies with latitude and time. At the time of solar maximum, our theoretical model gives negative helicity in the northern hemisphere and positive helicity in the south, in accordance with observed hemispheric trends. However, we find that during a short interval at the beginning of a cycle, helicities tend to be opposite of the preferred hemispheric trends.

Subject headings: MHD — Sun: activity — Sun: magnetic fields — sunspots

1. INTRODUCTION

It has been recognized for some time that solar active regions typically have some helicity associated with them and that the preferred sign of helicity in the two hemispheres are opposite (negative in the northern hemisphere and positive in the southern), in spite of a very large statistical scatter. Hale (1927) and Richardson (1941) noted the helical appearances of sunspots in Hα images. More systematic studies based on vector magnetogram data have been carried out by Seehafer (1990), Pevtsov et al. (1995, 2001), Abramenko et al. (1997), and Bao & Zhang (1998). Figure 2 of Canfield & Pevtsov (2000) is a typical plot showing a variation of helicity with latitude, which any theoretical model has to explain.

Solar magnetic fields are believed to be produced by the dynamo process. One possibility is that the dynamo process itself is responsible for the generation of helicity. The other possibility is that the rising flux tubes, which eventually form active regions, get the twist by interacting with the helical turbulence in the surrounding convection. The second possibility has been christened as the Σ-effect by Longcope et al. (1998), who investigated it (see also Longcope et al. 1999). Gilman & Charbonneau (1999) looked at the helicity generation by an interface dynamo. The two possibilities mentioned above need not be mutually exclusive: both may be simultaneously operative. A careful comparison between observational data and detailed theoretical models will be needed to ascertain the relative importance of these two effects. In fact, a recent analysis of observational data of solar active regions indicates that there must be some mechanism other than the Σ-effect, in the lower half of the solar convection zone, for the creation of helicity there (Holder et al. 2004).

We present here calculations of helicity based on our two-dimensional kinematic solar dynamo model presented in Nandy & Choudhuri (2002) and Chatterjee et al. (2004). In this dynamo model, the toroidal field is produced in the tachocline at the bottom of the convection zone, whereas the poloidal field is produced at the solar surface by the Babcock-Leighton process (i.e., from the decay of tilted bipolar regions). Since a meridional circulation, which advects the poloidal field first to high latitudes and then down to the tachocline, plays a crucial role in this model, we refer to this as a circulation-dominated solar dynamo model. The important role played by meridional circulation in such dynamo models was first demonstrated by Choudhuri et al. (1995) and Durney (1995). We have taken a meridional circulation penetrating slightly below the bottom of the solar convection zone (SCZ). This ensures that the toroidal field produced in the high-latitude tachocline (where the shear is strong) is carried through a stable layer to the low latitudes, where active regions are formed.

The dynamo equation deals with the mean magnetic field (see, for example, Choudhuri 1998, chap. 16), whereas we want to find helicities of active regions that form from flux tubes. To make a connection between these two, we have to look at the relation between dynamo theory and flux tubes. This has been explored by Choudhuri (2003), who presents the qualitative idea of how the helicity is generated. We recommend that the reader goes through § 5 of Choudhuri (2003) before reading this Letter, which develops the ideas outlined there. Basically, the toroidal and poloidal fields are generated in two different regions (at the bottom and at the top of the SCZ, respectively). When toroidal flux tubes move upward into the region near the solar surface where the poloidal field already exists, the poloidal field gets wrapped around the flux tube and gives rise to the helicity. This is explained through Figure 4 in Choudhuri (2003). In the northern hemisphere, when a flux tube rises in a region where a poloidal field has been created from *similar* flux tubes by the Babcock-Leighton process, this figure makes it clear that the helicity is negative (it has to be positive in the southern hemisphere).

We present an order-of-magnitude estimate of helicity in § 2 and show that it is in conformity with the observational data. Then the detailed results from the dynamo simulation are presented in § 3. Our conclusions are summarized in § 4.

2. ESTIMATING THE VALUE OF HELICITY

There are different ways of describing helicity mathematically, one of which is

$$\alpha = \frac{(\nabla \times \boldsymbol{B})_z}{B_z}, \tag{1}$$

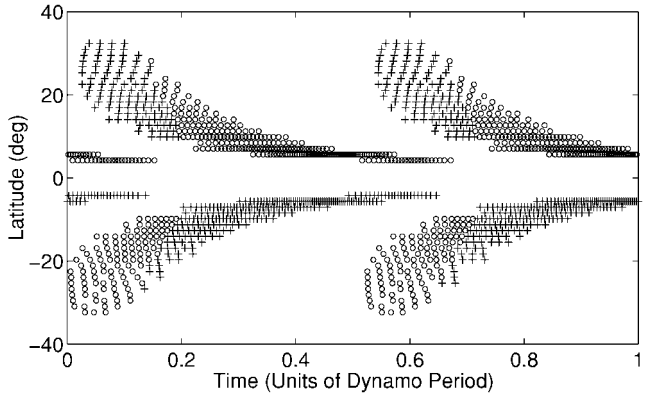

FIG. 1.—Theoretical butterfly diagram of eruptions from our standard dynamo model. Eruptions with positive and negative helicities are denoted by plus signs and circles, respectively.

where z corresponds to the vertical direction, which is along the axis of the flux tube for active regions on the surface. The parameter α (not to be confused with the dynamo α-effect traditionally associated with the poloidal field generation mechanism) is a measure of the twist in the magnetic field lines. The twist parameter is an indicator of how stressed the active region flux system is, and it is known to play an important role in the flaring and explosive activity of active region magnetic fields (Canfield et al. 1999; Nandy et al. 2003). Several authors calculated α for active regions from magnetogram data. Figure 2 of Canfield & Pevtsov (2000) plots α for the active regions against the latitudes where they are seen, clearly showing a statistical tendency for α to be negative in the northern and positive in the southern hemisphere, respectively. The typical observed value of the twist parameter α, as seen in this figure, is about 2×10^{-8} m^{-1}.

To estimate the value of helicity theoretically, we have to keep in mind that the flux of poloidal field B_P through the whole SCZ gets dragged by the toroidal flux tube rising under magnetic buoyancy (see Fig. 4 of Choudhuri 2003). If d is the depth of the convection zone, the flux dragged by the tube is

$$F \approx B_P d. \tag{2}$$

This flux F gets wrapped around the tube of radius a. In an ideal-MHD situation, this flux F would be confined to a narrow sheath around the flux tube. In reality, however, we expect that the turbulent disturbances around the flux tube would make this flux F penetrate into the flux tube to some extent. Then the magnetic field going around the tube can be taken to be of order F/a. The current density $|\nabla \times \boldsymbol{B}|$ associated with this field is of order F/a^2 and is along the axis of the tube. If B_T is the magnetic field inside the flux tube, then it follows from equation (1) that

$$\alpha \approx \frac{F/a^2}{B_T} \approx \frac{B_P d}{B_T a^2} \tag{3}$$

on substituting from equation (2) for F. We use $B_P \approx 1$ G, the depth of the SCZ $d \approx 2 \times 10^8$ m, and the field inside sunspots $B_T \approx 3000$ G. On taking the radius of the sunspot $a \approx 2000$ km and $a \approx 5000$ km, we get $\alpha \approx 2 \times 10^{-8}$ m^{-1} and $\alpha \approx 3 \times 10^{-9}$ m^{-1}, respectively. Thus, from very simple arguments, we get the correct order of magnitude. This suggests that our model captures some amount of the real physics. If the flux F that is wrapped around the flux tube is confined to a shell of thickness less than a (i.e., is not spread over the full radius), then the current density also would be confined in the shell and would have a value higher than F/a^2, making α higher than what is estimated above. Using a fixed value of α to describe the helicity of a sunspot is certainly an oversimplification from either a theoretical or an observational point of view.

3. RESULTS FROM SIMULATION

In § 4 of Chatterjee et al. (2004), we have presented a particular dynamo model, which we refer to as our *standard model*. This model settles into a solution with dipolar parity, produces a butterfly diagram that matches with observations, and gives the correct phase relation between sunspots and weak fields outside active regions. We now present helicity calculations based on this standard model. Full details of the model are given in Chatterjee et al. (2004).

For simplicity, let us assume that all flux tubes have the same radius a. It then follows from equation (3) that the helicity of the flux tube is essentially given by the flux F through the SCZ. A flux eruption takes place in our model whenever the toroidal field at the bottom of the SCZ exceeds a critical value. Details of how we do this are discussed in Nandy & Choudhuri (2001) and are summarized in § 2.6 of Chatterjee et al. (2004). Whenever an eruption takes place in our dynamo simulation, we calculate the poloidal flux F through the SCZ at the eruption latitude by integrating B_θ from the bottom of the SCZ ($r = R_b$) to the top ($r = R_\odot$), i.e.,

$$F = \int_{R_b}^{R_\odot} B_\theta \, dr.$$

Since the poloidal field is obtained from a scalar function $A(r, \theta)$ by the relation $\boldsymbol{B}_p = \nabla \times (A\boldsymbol{e}_\phi)$, it is easy to see that

$$F = -\left[A(r = R_\odot) + \int_{R_b}^{R_\odot} \frac{A}{r} \, dr\right]. \tag{4}$$

The value of F calculated at the eruption latitude at the time of eruption gives the amplitude of helicity associated with the eruption. The sign is obtained from the following convention: if the sign of F is opposite to the sign of the toroidal field B at the bottom of the SCZ, then the helicity is taken as negative (otherwise it is positive). This should be clear from a perusal of Figure 4 of Choudhuri (2003).

Figure 1 shows the simulated butterfly diagram, indicating active regions of positive and negative helicity. During the solar maximum, the helicity is negative in the northern hemisphere and positive in the southern, as we expect. However, at the beginning of a cycle, there is a short duration when the sign of helicity is "wrong," i.e., opposite of the preferred helicity. Basically, when a flux tube erupts in a region where the poloidal field has been created by *similar* flux tubes that erupted earlier, we get the "correct" (i.e., preferred) helicity. At the beginning of a cycle, flux tubes emerge in regions where the poloidal field was produced by flux tubes of the earlier cycle, thereby giving rise to "wrong" helicity. We find that 67% of the eruptions in our simulation have "correct" helicity. This percentage, however, depends on the parameters of the model. By varying parameters, we have succeeded in producing cases in which 78% of the eruptions have "correct" helicity, although the butterfly diagrams for these cases match observations less well. We are now in the process of introducing stochastic fluctuations

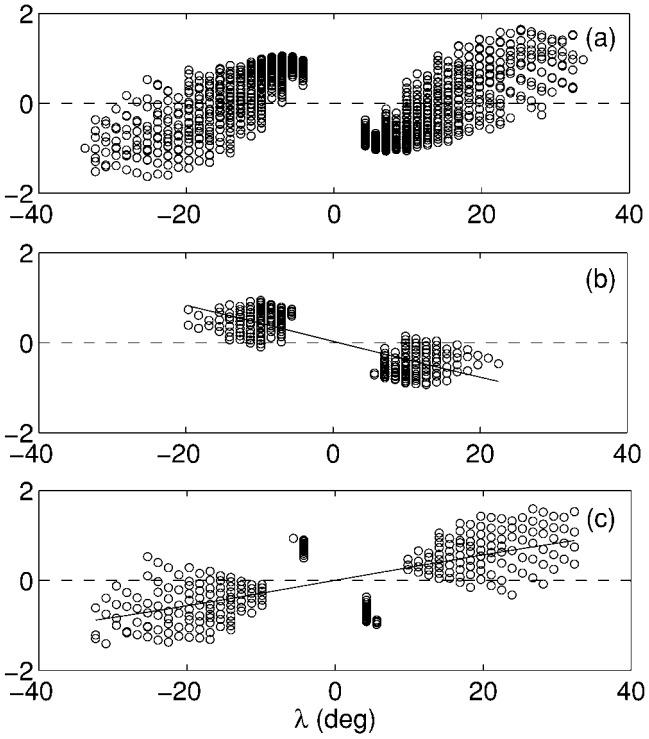

FIG. 2.—Helicity α (plotted along the vertical axis in arbitrary units) for eruptions at different latitudes, denoted by open circles: (*a*) for an entire solar cycle; (*b*) for 4 years during the maximum and the declining phases of the solar cycle; and (*c*) for the first 4 years of the solar cycle. The solid lines in (*b*) and (*c*) are least–squares fits to the model results.

in our dynamo model, which is needed to model the irregularities of the solar cycle. The helicity results obtained with our present regular dynamo code also may get slightly modified on introducing the stochastic fluctuations. We plan to carry out a more complete parameter space study after incorporating the fluctuations.

In an analysis of solar active region data, Bao et al. (2000) find evidence that, during the beginning of Cycle 23, the current helicity (an alternative parameter to describe helicity) had the opposite of the preferred sign, lending support to our preliminary theoretical results. However, Pevtsov et al. (2001) do not find such a reversal in their analysis of active region data from the first 4 years of Cycle 23, and Bao et al. (2000) also do not find this reversal in the α parameter. More detailed analyses of both observational data and theoretical models are clearly needed.

Figure 2*a* is a plot of helicity associated with eruptions at different latitudes. This is the theoretical plot that has to be compared with observational plots like Figure 2 of Canfield & Pevtsov (2000). We notice that the theoretical plot has considerably less scatter compared to the observational data. This is expected to change on introducing stochastic fluctuations, which should increase the scatter. However, even the present model without stochastic fluctuations reproduces the broad features of observational data reasonably well.

To see the variation of helicity with the cycle, Figures 2*b* and 2*c* present plots of helicity for eruptions during 4 years of solar maximum and 4 years at the beginning of the cycle, respectively. The straight lines represent the least-squares fits. For "correct" helicity (negative in north and positive in south), the gradient $d\alpha/d\lambda$ of the straight line has to be negative, as we see in Figure 2*b* corresponding to solar maximum (λ is the

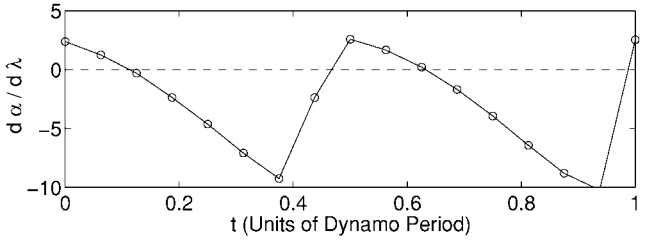

FIG. 3.—$d\alpha/d\lambda$ as a function of time covering the equivalent of two sunspot cycles. To find out the values of time that correspond to maxima or minima, look at Fig. 1, which has the same horizontal axis.

latitude). The gradient, however, is positive at the start of the cycle. To find out how this gradient varies with the cycle, we divide the cycle period into 16 equal intervals and then find the gradient $d\alpha/d\lambda$ for each of the intervals by using eruptions during that interval. Figure 3 shows how the gradient $d\alpha/d\lambda$ varies with the solar cycle. If the Σ-effect makes a significant contribution in the production of helicity, then the variation with the cycle may be less pronounced compared to what we find in our model without this effect, since the Σ-effect is cycle independent (Longcope et al. 1998).

Since it is in principle possible to determine from observational data how $d\alpha/d\lambda$ actually varies with the solar cycle, a plot like Figure 3 provides a powerful tool for comparison between theory and observations. There is some indication in the existing data that $d\alpha/d\lambda$ may be varying in accordance with our model; but the data are noisy and the results from different instruments often diverge widely, so it is difficult to draw firm conclusions at this point in time (A. A. Pevtsov 2004, private communication).

4. CONCLUSION

We have shown how helicity can be calculated from a dynamo model. There are different mathematical ways of describing helicity. We have made use of the parameter α defined through equation (1). Another way of describing it is through the magnetic helicity $\boldsymbol{A}\cdot\boldsymbol{B}$. It is well known that magnetic helicity changes much more slowly than magnetic energy (see, for example, Choudhuri 1998, § 15.3). It has been suggested that the dynamo creates magnetic helicities of opposite signs at the large and small scales so that there is no net change in magnetic helicity (Seehafer 1996; Blackman & Brandenburg 2003). The α-effect associated with the dynamo (different from α defined in eq. [1]) is positive in the northern hemisphere and produces positive helicity of the mean field (see the Appendix of Choudhuri 2003). Choudhuri (2003, § 5.2) has explained how positive helicity is produced in the large scale, with a simultaneous generation of negative helicity at small scales to be identified with the helicity of active regions. These subtle issues were not recognized in the early attempts of calculating helicity from dynamo models (Gilman & Charbonneau 1999).

Two clear theoretical predictions follow from our model:

1. Since the helicity goes as a^{-2} as seen from equation (3), the smaller sunspots should statistically have stronger helicity (i.e., higher values of twist α).
2. At the beginning of a cycle, helicity should be opposite of what is usually observed.

The alternative model for the generation of helicity, the Σ-effect proposed by Longcope et al. (1998), also makes the prediction 1 but not 2. Since helicity is imparted to the flux

tubes by helical turbulence of the SCZ in this model, the helicity is not expected to vary with the solar cycle. A careful analysis of any possible variation of helicity with the solar cycle would be the best way of ascertaining relative contributions of the Σ-effect and the dynamo (the process studied in this Letter) in generating helicity. As already noted, Bao et al. (2000) noticed indications of opposite helicity at the beginning of Cycle 23 in conformity with our preliminary theoretical results, although other groups have not confirmed this result. More careful analysis of observational data is needed to establish any possible cycle dependence of helicity. We hope that this will be done in the near future. Also, there are indications in observational data that helicities of "wrong" sign—that do not follow the hemispheric trend—often persist at certain latitudes and longitudes over several months (see Pevtsov & Balasubramaniam 2003 for a review of such *helicity nests*). More complicated theoretical models, perhaps with stochastic fluctuations and departures from axisymmetry, will be needed to explain these details.

Most of our calculations were carried out on the parallel cluster computer at the Centre for High Energy Physics, Indian Institute of Science. D. N. acknowledges financial support from NASA through Supporting Research and Technology grant NAG5-11873. P. C. acknowledges the Council of Scientific and Industrial Research for financial support. We thank the anonymous referee for constructive suggestions.

REFERENCES

Abramenko, V. I., Wang, T., & Yurchishin, V. B. 1997, Sol. Phys., 174, 291
Bao, S., Ai, G. X., & Zhang, H. 2000, J. Astrophys. Astron., 21, 303
Bao, S., & Zhang, H. 1998, ApJ, 496, L43
Blackman, E. G., & Brandenburg, A. 2003, ApJ, 584, L99
Canfield, R. C., Hudson, H. S., & McKenzie, D. E. 1999, Geophys. Res. Lett., 26, 627
Canfield, R. C., & Pevtsov, A. A. 2000, J. Astrophys. Astron., 21, 213
Chatterjee, P., Nandy, D., & Choudhuri, A. R. 2004, A&A, in press (astro-ph/0405027)
Choudhuri, A. R. 1998, The Physics of Fluids and Plasmas: An Introduction for Astrophysicists (Cambridge: Cambridge Univ. Press)
———. 2003, Sol. Phys., 215, 31
Choudhuri, A. R., Schüssler, M., & Dikpati, M. 1995, A&A, 303, L29
Durney, B. R. 1995, Sol. Phys., 160, 213
Gilman, P. A., & Charbonneau, P. 1999, in Magnetic Helicity in Space and Laboratory Plasmas, ed. M. R. Brown, R. C. Canfield, & A. A. Pevtsov (Geophys. Monogr. 111; Washington, DC: AGU), 75
Hale, G. E. 1927, Nature, 119, 708
Holder, Z. A., Canfield, R. C., McMullen, R. A., Nandy, D., Howard, R. F., & Pevtsov, A. A. 2004, ApJ, 611, 1149
Longcope, D. W., Fisher, G. H., & Pevtsov, A. A. 1998, ApJ, 507, 417
Longcope, D. W., Linton, M., Pevtsov, A., Fisher, G., & Klapper, I. 1999, in Magnetic Helicity in Space and Laboratory Plasmas, ed. M. R. Brown, R. C. Canfield, & A. A. Pevtsov (Geophys. Monogr. 111; Washington, DC: AGU), 93
Nandy, D., & Choudhuri, A. R. 2001, ApJ, 551, 576
———. 2002, Science, 296, 1671
Nandy, D., Hahn, M., Canfield, R. C., & Longcope, D. W. 2003, ApJ, 597, L73
Pevtsov, A. A., & Balasubramaniam, K. S. 2003, Adv. Space Res., 32, 1867
Pevtsov, A. A., Canfield, R. C., & Latushko, S. M. 2001, ApJ, 549, L261
Pevtsov, A. A., Canfield, R. C., & Metcalf, T. R. 1995, ApJ, 440, L109
Richardson, R. S. 1941, ApJ, 93, 24
Seehafer, N. 1990, Sol. Phys., 125, 219
———. 1996, Phys. Rev. E, 53, 1283